

Provided for non-commercial research and education use.  
Not for reproduction, distribution or commercial use.



This article appeared in a journal published by Elsevier. The attached copy is furnished to the author for internal non-commercial research and education use, including for instruction at the authors institution and sharing with colleagues.

Other uses, including reproduction and distribution, or selling or licensing copies, or posting to personal, institutional or third party websites are prohibited.

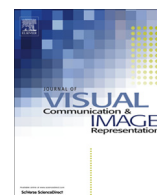
In most cases authors are permitted to post their version of the article (e.g. in Word or Tex form) to their personal website or institutional repository. Authors requiring further information regarding Elsevier's archiving and manuscript policies are encouraged to visit:

<http://www.elsevier.com/authorsrights>



Contents lists available at SciVerse ScienceDirect

J. Vis. Commun. Image R.

journal homepage: [www.elsevier.com/locate/jvcir](http://www.elsevier.com/locate/jvcir)

## Geometric and colorimetric error compensation for multi-view images



Jae-Il Jung, Yo-Sung Ho\*

Gwangju Institute of Science and Technology (GIST), 123 Cheomdangwagi-ro, Buk-gu, Gwangju 500-712, South Korea

### ARTICLE INFO

#### Article history:

Available online 20 April 2013

#### Keywords:

Multi-view image  
Geometric compensation  
Color correction  
Uniform view interval  
Vertical disparity reduction  
Projective transformation  
Visual fatigue  
3DTV

### ABSTRACT

In general, excessive colorimetric and geometric errors in multi-view images induce visual fatigue to users. Various works have been proposed to reduce these errors, but conventional works have only been available for stereoscopic images while requiring cumbersome additional tasks, and often showing unstable results. In this paper, we propose an effective multi-view image refinement algorithm. The proposed algorithm analyzes such errors in multi-view images from sparse correspondences and compensates them automatically. While the conventional works transform every view to compensate geometric errors, the proposed method transforms only the source views with consideration of a reference view. Therefore this approach can be extended regardless of the number of views. In addition, we also employ uniform view intervals to provide consistent depth perception among views. We correct color inconsistency among views from the correspondences by considering importance and channel properties. Various experimental results show that the proposed algorithm outperforms conventional approaches and generates more visually comfortable multi-view images.

© 2013 Elsevier Inc. All rights reserved.

### 1. Introduction

Following the significant advances in three-dimensional (3D) display technologies and fast network services, we can now easily access immersive image data at home. Recent 3D video services are based on the stereoscopic image which provides binocular parallax by presenting two offset images separately. However, the stereoscopic image allows viewers to perceive depth impression at only a fixed viewpoint.

The multi-view image, the extension of the stereoscopic image, was proposed to increase available viewpoints [1]. These are captured by multiple cameras (generally more than two) at different positions. Some industries have developed prototypes of multi-view display devices that are able to simultaneously present multiple images at different viewpoints [2,3]. Fig. 1 shows the difference between stereoscopic and multi-view image systems. Such multi-view images additionally provide motion parallax unlike stereoscopic images.

The visual quality of multi-view images depends not only on the individual image qualities but also the relative properties among views such as relative color distribution and geometric arrangement. However, captured multi-view images exhibit geometric and colorimetric errors in most cases since manual adjustment of multiple cameras are very difficult.

In multi-view camera systems, the captured color distribution of a certain object depends on the reflectance property of the object as well as camera properties. Therefore, the color distribution of each camera may vary regardless of the same capturing environ-

ment. This phenomenon is called color inconsistency among views; this is inevitable even with same kind of cameras.

A certain point in the real world is projected to different positions on multi-view image planes. These disparities can be categorized in two directions. Horizontal disparities are deeply involved in depth perception while vertical disparities disturb the fusion phenomenon in the human visual system. Now that the display devices present multiple views to equally spaced regions as shown in Fig. 1, the multi-view image provides different depth perception among views if view intervals are irregular.

Humans are known to have a tolerance to small geometric or colorimetric errors in multi-view images; however viewers may complain visual fatigue when exposed to error-prone 3D contents for hours [4–6]. Therefore, compensation of the colorimetric and geometric errors is important for providing comfortable multi-view contents to viewers.

In relation of colorimetric error in multi-view images, the most common approaches are based on a known color chart [7]. Such methods estimate multiple camera responses by analyzing the color patches of the captured chart and compensate color distributions. These approaches show reliable results but require cumbersome task of capturing the color chart for every scene. In addition, owing to this task, we cannot apply these algorithms to general multi-view images captured without the color chart.

For resolving this problem, color correction algorithms based on global image properties have been suggested. Reinhard et al. proposed a linear transformation from statistical analysis to impose color distribution of one image to another [8]. This statistical model has been widely used as the baseline of other color correction

\* Corresponding author. Fax: +82 62 715 3164.

E-mail address: [hoyo@gist.ac.kr](mailto:hoyo@gist.ac.kr) (Y.-S. Ho).

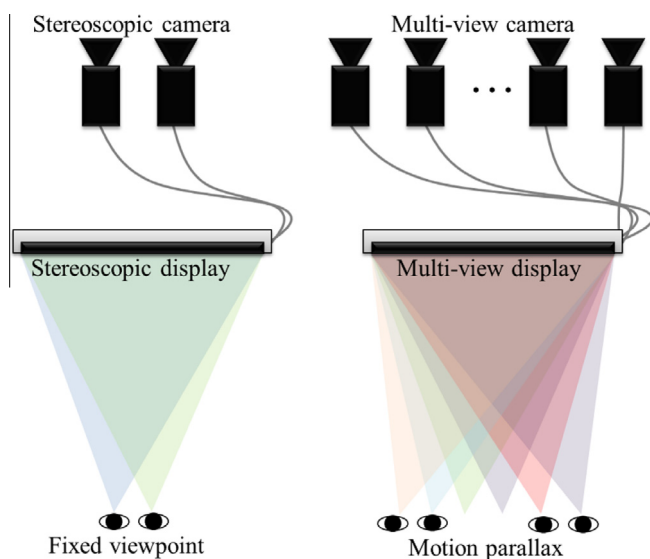


Fig. 1. Stereoscopic and multi-view image systems.

approaches. Frecker et al. correct color distribution using cumulative color histogram for calculating mapping relation between two images [9]. Since these methods do not consider occlusion regions which are newly exposed areas due to the viewpoint difference, their performance highly depends on the portion of these regions in input images.

In order to reduce the influence of occlusion regions, recent approaches use correspondences between views. Yamamoto et al. and Panahpour et al. use an energy function (EF) for reducing color differences between correspondence pairs [10,11]. This method successively avoids the occlusion problem, but sometimes the energy terms in EF conflict inducing distortions in homogeneous regions. Kim et al. suggested likelihood maximization for estimation of the brightness transfer function (BTF), exposure, and vignetting [12]. Wang et al. proposed an algorithm for correcting colors region-by-region [13], using a color segmentation method to divide regions and correct colors locally. Jung et al. suggested a relative camera characteristic model between views, which considers camera properties, but its performance depends on the quality of correspondences [14]. While these algorithms solve the occlusion problem, their performance is unstable for various scenes.

Related to the geometric error, the most effective way to improve the geometric alignment is multi-view rectification using camera parameters, proposed by Kang et al. [15]. This approach calculates exact transformation matrices for multi-view images with consideration of intrinsic properties and relative camera position and rotation. Although this method efficiently aligns multi-view image planes and makes view intervals uniform, the use is limited to only the case where all cameras are calibrated. Camera

calibration contains complex tasks such as capturing a grid pattern board, extracting feature points, and estimating parameters. In addition, all cameras should be calibrated again whenever cameras movements including panning, tilting, and zooming happen.

Image rectification is the most famous method for reducing vertical disparities without camera parameters. This process makes all epipolar lines parallel in input image pairs [16]. In general, the fundamental matrix is used to estimate transformation matrices for image pairs and can be easily estimated from correspondences [17]. Although we can reduce vertical disparities between image pairs using image rectification, sometimes this process severely distorts input images. Several constraints have been researched to reduce distortion [18,19] but this still remains problematic.

The other problem is that we cannot apply image rectification to multi-view images since image rectification transforms all input views. Now that we have many views to be rectified in multi-view images, rectified image pair goes wrong if one view in the pair is rectified with the other view. Nozick proposed image rectification method for multi-view images that considers all views, but its performance is not stable since this method only uses scaling and Euler angles to rectify images [20]. In addition, the mentioned methods do not consider view intervals between views. Uniform view intervals are very important since multi-view display devices independently present different views to uniformly divided areas as shown in Fig. 1. The multi-view image provides different depth perception among views if view intervals are irregular.

In this paper, we propose a multi-view image refinement algorithm that successively align multiple views and correct color distributions. The proposed method reduces vertical disparities of multi-view images and also makes horizontal view intervals uniform. In addition, the proposed method includes a color correction algorithm using adaptive weights of correspondences. These two corrections enhance viewing comfort and guarantee similar depth impression among views in multi-view contents through multi-view display devices.

There are some other works to compensate geometric and colorimetric errors for projected images and tiled projects [21–23], but the goals and approaches are different from our approach. The errors from the conventional works come from the characteristics of single-view camera or projectors, but the errors in multi-view images are induced due to the relative differences of multiple cameras. Therefore, approaches and solutions are also different. In this paper, we focus on the errors in multi-view images.

The remainder of this paper is organized as follows: In Section 2, we introduce the proposed algorithm in detail. The effectiveness of our algorithm is compared to other approaches in Section 3. Then, this paper concludes in Section 4.

## 2. Compensating geometric and colorimetric errors

The proposed algorithm modifies color distribution and alignment of source views ( $V_s$ ), with respect to a reference view ( $V_r$ )

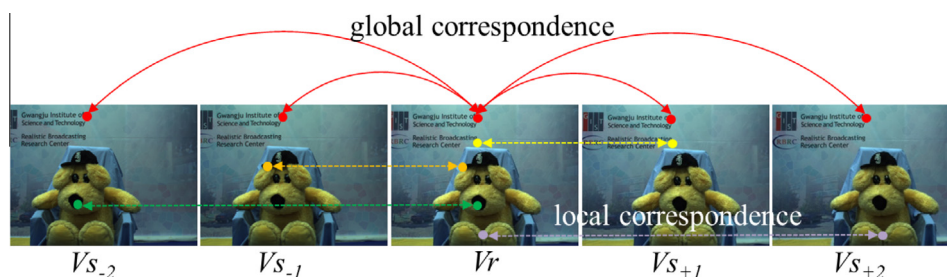


Fig. 2. Reference ( $V_r$ ) and source ( $V_s$ ) views. Red arcs represent global correspondences and the dotted lines show local correspondences between view pairs. (For interpretation of the references to colour in this figure legend, the reader is referred to the web version of this article.)

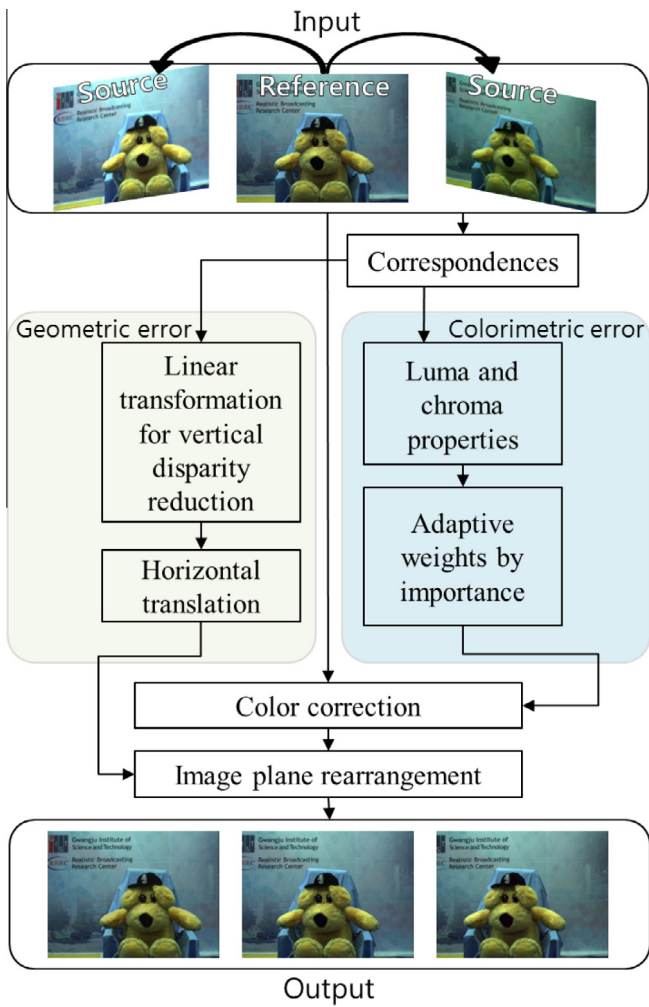


Fig. 3. Overall procedure of the proposed algorithm.

in consecutive order. The center view is generally selected as a reference view, but we can select the other view as a reference view accordingly. The compensation process independently works in pairs. In the proposed method, we use two types of correspondences to analyze differences among views: global and local correspondences. Global correspondences are common features on all

views. On the contrary, local correspondences are matched features for a certain pair as shown in Fig. 2.

In order to extract correspondences, we adopt the Speed Up Robust Feature (SURF) [24]. Outliers in the extracted correspondences are removed by Random Sample Consensus (RANSAC) [25]. Fig. 3 shows the overall procedure of the proposed algorithm. After estimating colorimetric and geometric compensation parameters independently, we correct colors and realign image planes of multi-view images.

### 2.1. Geometric error compensation

Due to the difficulty of perfectly aligning multiple cameras at desired viewpoints with desired angles, the captured multi-view images generally have unwanted vertical disparities and non-uniform view intervals. In order to improve the alignment of multi-view image planes, we rearrange the image planes of source views with consideration of the reference view. While the conventional rectification distorts both source and reference view, the proposed method only transforms source views as shown in Fig. 4. This approach allows us to compensate the geometric errors of multiple views in consecutive order.

Linear transformation represented by a non-singular  $3 \times 3$  matrix is used to transform source views. If the camera parameters are available, it is straightforward to calculate the matrix; however, these parameters are generally not available in practice. Therefore, we approximate this matrix from the correspondences in two stages: vertical disparity reduction and horizontal translation. The projective transformation generally used in computer vision has nine components with eight degrees of freedom as

$$\mathbf{x}'_s = \mathbf{H}\mathbf{x}_s = \begin{bmatrix} a_{11} & a_{12} & t_x \\ a_{21} & a_{22} & t_y \\ v_1 & v_2 & 1 \end{bmatrix} \mathbf{x}_s \quad (1)$$

$\mathbf{x}_s$  is a pixel in homogeneous coordinates  $(x, y, w)$  of the source view, and  $\mathbf{x}'_s$  is the transformed position by the linear transformation  $\mathbf{H}$ . The  $a$  components are for camera rotation and deformation, the  $t$  components are for translation, and  $v$  components are related to projective properties. Since estimation of many unknown parameters is not, we limit and combine some parameters to reduce the number of unknowns. The matrix  $\mathbf{A}$  consisting of  $a$  components can be decomposed as

$$\mathbf{A} = \begin{bmatrix} a_{11} & a_{12} \\ a_{21} & a_{22} \end{bmatrix} = \mathbf{R}(\theta)\mathbf{R}(-\phi)\mathbf{Z}\mathbf{R}(\phi) \text{ where } \mathbf{Z} = \begin{pmatrix} z_x & 0 \\ 0 & z_y \end{pmatrix} \text{ and } \mathbf{R}(\alpha) = \begin{pmatrix} \cos \alpha & -\sin \alpha \\ \sin \alpha & \cos \alpha \end{pmatrix} \quad (2)$$

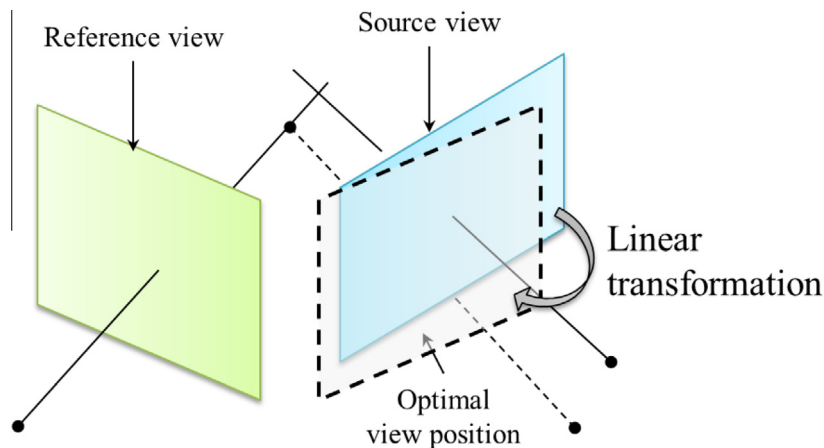


Fig. 4. One side correction for geometric error reduction.

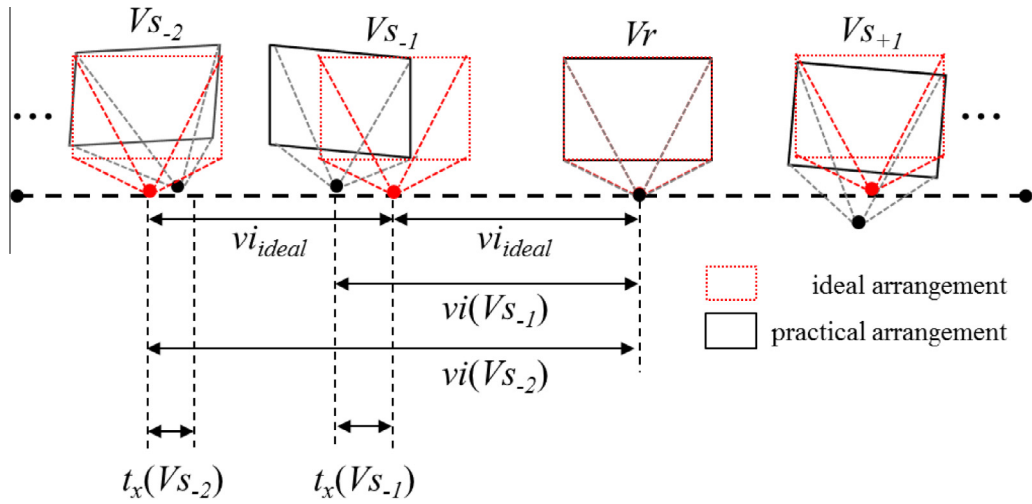


Fig. 5. Relation between ideal and practical view arrangements.

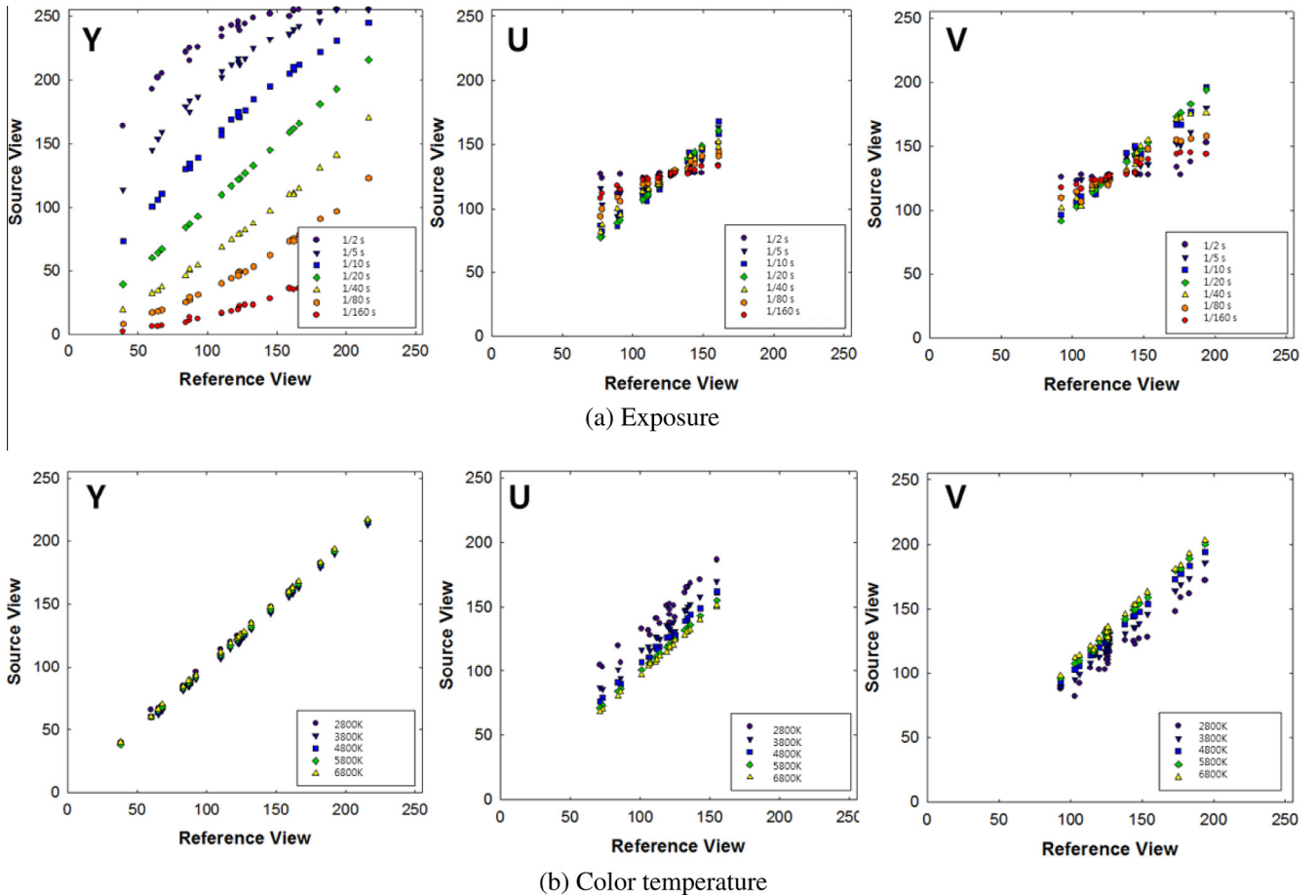


Fig. 6. Corresponding relation between views in the YUV color domain. (For interpretation of the references to colour in this figure legend, the reader is referred to the web version of this article.)

The parameters  $\theta$  and  $\phi$  are angles for image rotation and deformation, respectively.  $z_x$  and  $z_y$  are for scaling in the  $x$ - and  $y$ -direction. Since two directional scaling is meaningless to our goal, we combine  $z_x$  and  $z_y$  into a scalar value  $z$ , which compensates a different zooming effect between reference and source views. When replacing the matrix  $\mathbf{Z}$  with the scalar value  $z$ , we can simply (2) as

$$\mathbf{A}' = z\mathbf{R}(\theta)\mathbf{R}(-\phi)\mathbf{R}(\phi) = z \begin{bmatrix} b_1 & b_2 \\ -b_2 & b_1 \end{bmatrix} = \begin{bmatrix} zb_1 & zb_2 \\ -zb_2 & zb_1 \end{bmatrix} = \begin{bmatrix} m_1 & m_2 \\ -m_2 & m_1 \end{bmatrix} \quad (3)$$

where  $b_1 = \cos\phi\cos\theta\cos(-\phi) - \cos\phi\sin\theta\sin(-\phi) - \sin\phi\cos\theta\sin(-\phi) - \sin\phi\sin\theta\cos(-\phi)$  and  $b_2 = -\sin\phi\cos\theta\cos(-\phi) - \sin\theta\sin(-\phi)\sin\phi - \cos\phi\cos\theta\sin(-\phi) + \cos\phi\sin\theta\cos(-\phi)$ . In the last term,  $m_1 = zb_1$  and  $m_2 = zb_2$ . With this simplification, we can reduce the number of parameters to be estimated from four ( $a_{11}$ ,  $a_{12}$ ,  $a_{21}$ , and  $a_{22}$ ) to two ( $m_1$  and  $m_2$ ) for matrix  $\mathbf{A}'$ . In addition, we only consider vertical translation  $t_y$  at this step, since horizontal translation  $t_x$  does not affect vertical disparity reduction.  $t_x$  will be estimated at the

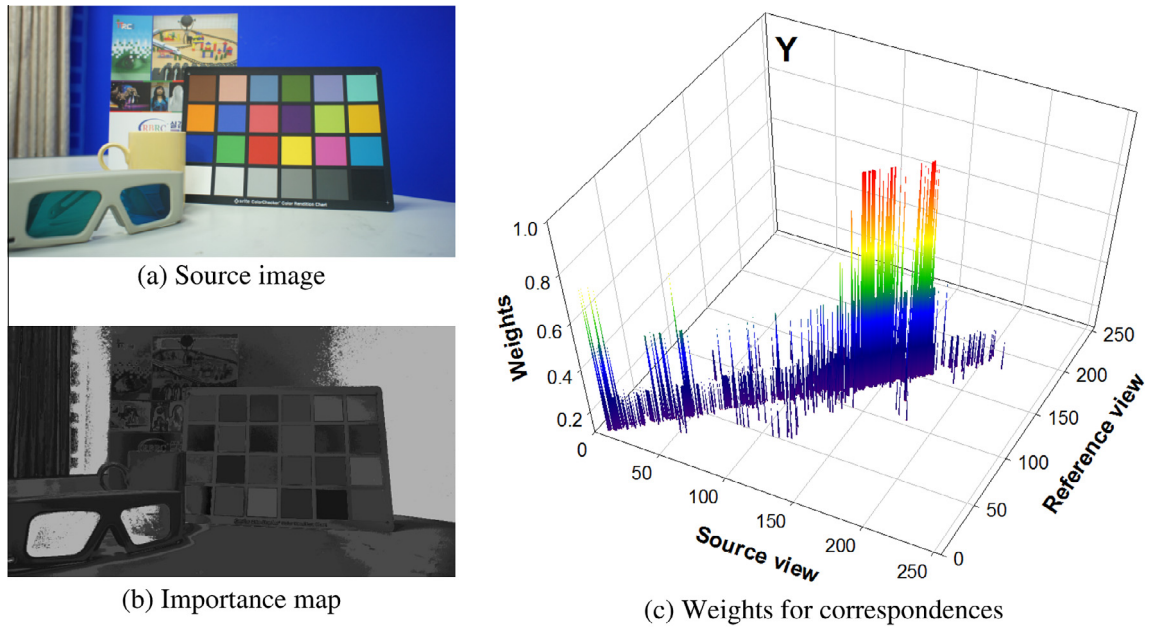


Fig. 7. Adaptive weights for correspondences according to importance.

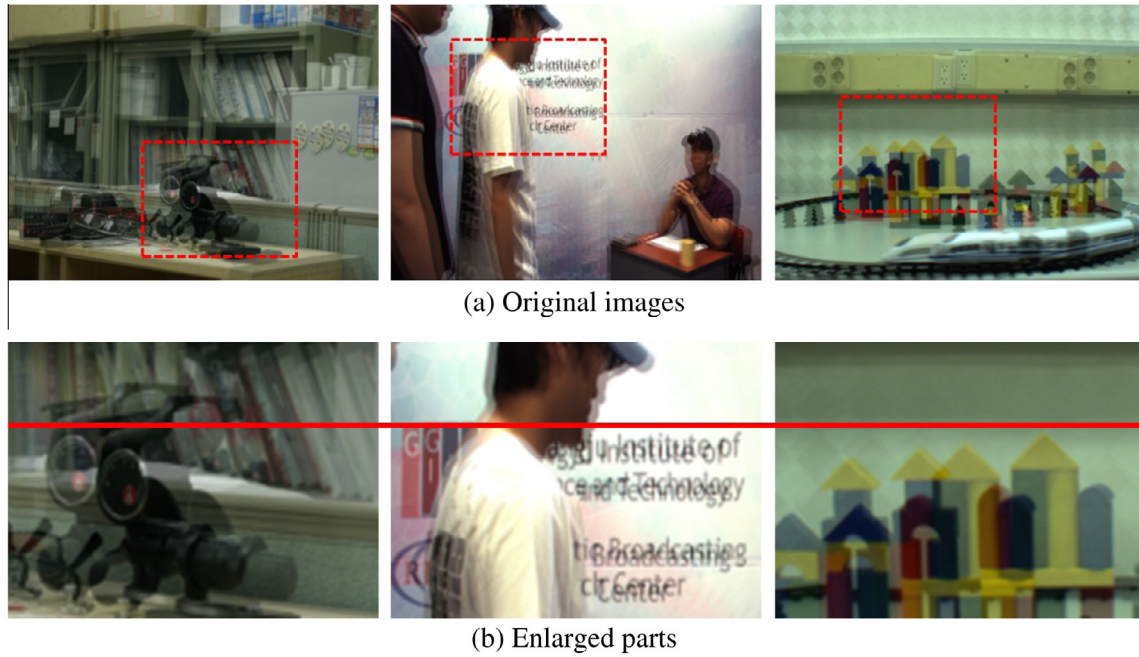


Fig. 8. Overlapped images of reference and source views.

next stage. Consequentially, the transformation matrix  $\mathbf{H}_{vd}$  for vertical disparity reduction has five degrees of freedom, and is expressed as

$$\mathbf{H}_{vd} = \begin{bmatrix} m_1 & m_2 & 0 \\ -m_2 & m_1 & t_y \\ v_1 & v_2 & 1 \end{bmatrix} \quad (4)$$

These five unknowns are estimated so that  $\mathbf{H}_{vd}$  reduces vertical disparities while minimizing distortion of the source view. We only consider a set of correspondences  $\mathbf{x}_{si} = (x_{si}, y_{si}, w_{si})^T \leftrightarrow \mathbf{x}_{ri} = (x_{ri}, y_{ri}, w_{ri})^T$  for minimizing the error function expressed as

$$Error_{vd} = \sum_{i=1}^N \left( \frac{y_{ri}}{w_{ri}} - \frac{y'_{si}}{w'_{si}} \right)^2 + \left| \frac{x_{si}}{w_{si}} - \frac{x'_{si}}{w'_{si}} \right| \quad (5)$$

where  $N$  represents the number of the correspondences and  $\mathbf{x}'_{si} = \mathbf{H}_{vd}\mathbf{x}_{si}$ . The first term is for vertical disparity reduction, and the second term is for constraint minimizing horizontal movement of source views. Since vertical alignment is the higher priority, we use squared summation for this term. The estimated homography  $\mathbf{H}_{vd}$  is the one for which the error is minimized via the Levenberg–Marquardt (LM) algorithm [26].

After estimating  $\mathbf{H}_{vd}$ , we find the horizontal translation  $t_x$  in order to make view intervals uniform considering global

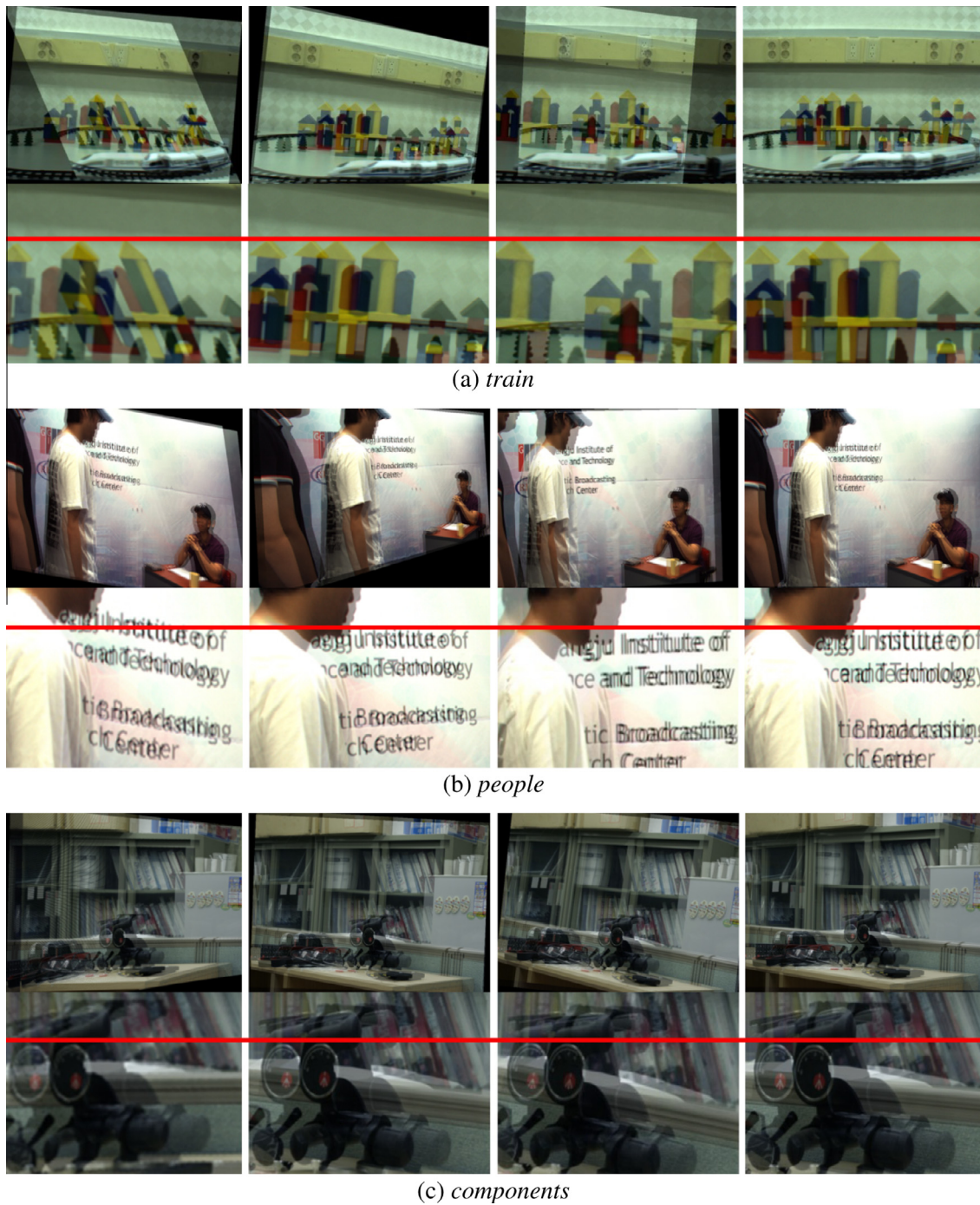


Fig. 9. Results of geometric error reduction: Hartley's, Fusiello's, Nozick's, and the proposed algorithms.

Table 1

Averages of vertical disparities of correspondences.

Test image	Original	Hartley's	Fusiello's	Nozick's	Proposed
Train	11.93	0.84	2.58	1.27	1.37
People	4.78	1.62	1.83	2.59	1.68
Components	11.49	0.76	1.59	1.40	1.09

correspondences. Fig. 5 shows the relation between ideal and practical arrangements.

$vi(Vs)$  represents the view interval between  $Vs$  and  $Vr$ , and  $vi_{ideal}$  means the ideal interval between neighboring views. We define

$vi_{ideal}$  so that movements on the horizontal direction of all views are minimized as

$$\begin{aligned}
 vi_{ideal}^* &= \arg \min_{vi_{ideal}} \sum_{vn} t_x^2(Vs_{vn}), \quad \text{where } t_x(Vs_{vn}) \\
 &= ||vn|vi_{ideal} - v_{vn}(Vs_{vn})|
 \end{aligned} \tag{6}$$

where  $vn$  represents the relative view number with respect to  $Vr$ , and  $t_x(Vs)$  is the horizontal movement of  $Vs$  when  $vi_{ideal}$  is given.  $vi(Vs)$  is the average view interval of the transformed correspondences  $\mathbf{x}_s^*$  between  $Vs$  and  $Vr$ . We can minimize the summation in (6) using the 1st derivative owing to the property of the quadric function. After that, we can get the final transformation matrix as

**Table 2**  
Comparison of valid pixel and valid viewing region.

Test image	Valid pixel (%)				Valid viewing region (%)			
	Hartley's	Fusiello's	Nozick's	Proposed	Hartley's	Fusiello's	Nozick's	Proposed
Train	56.37	76.81	68.02	99.00	33.27	62.82	58.07	97.68
People	73.91	70.62	88.36	99.47	68.48	51.75	84.23	98.87
Components	79.69	93.12	87.97	97.91	70.11	80.84	79.01	97.17

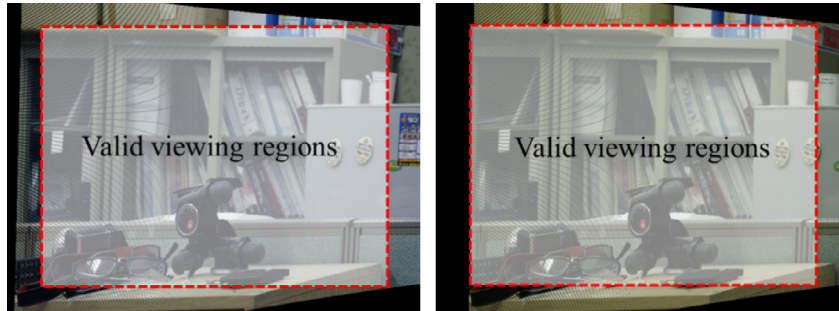


Fig. 10. Valid viewing region after cropping.

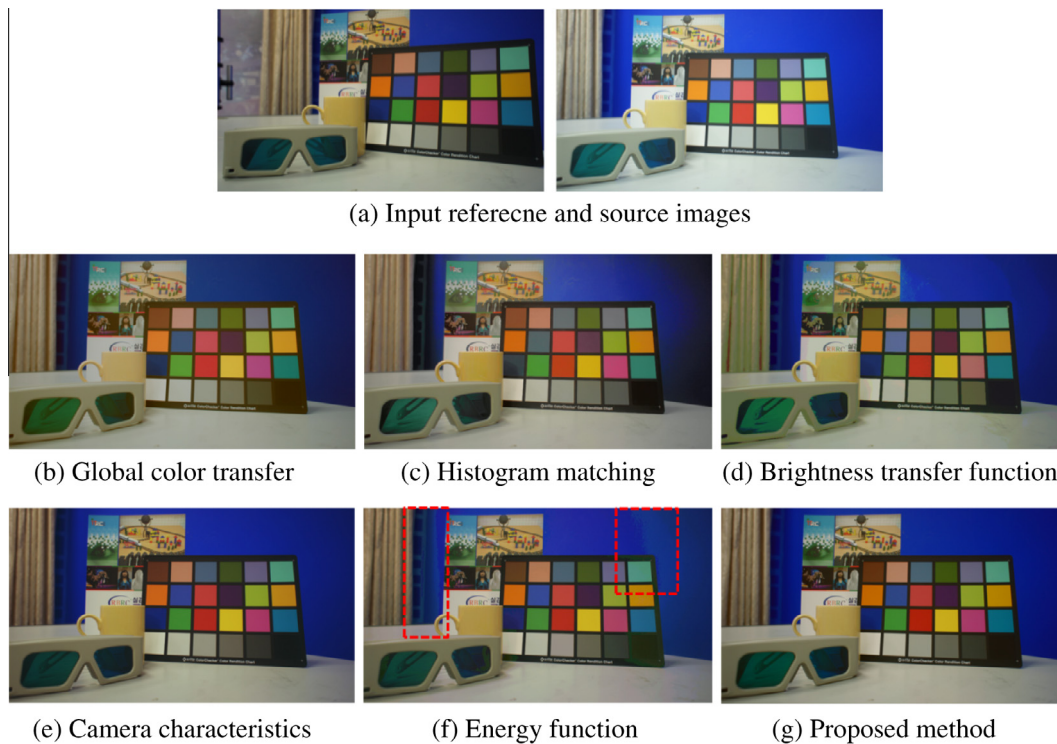


Fig. 11. Results of color correction: input images and results. (For interpretation of the references to colour in this figure legend, the reader is referred to the web version of this article.)

**Table 3**  
Comparison of color correction results.

Color correction	MSE			ED
	$L$	$a$	$b$	
Global color transfer	18.71	6.83	9.00	22.89
Histogram matching	17.13	7.13	6.79	21.16
Brightness transfer function	18.46	8.08	7.79	22.03
Camera characteristic	5.46	1.67	1.50	6.45
Energy function	2.43	0.70	1.18	2.79
Proposed	1.60	0.89	1.83	2.59

$$\mathbf{H}_{fm} = \begin{bmatrix} m_1 & m_2 & t_x \\ -m_2 & m_1 & t_y \\ v_1 & v_2 & 1 \end{bmatrix} \quad (7)$$

Afterwards, each source view is transformed by its own  $\mathbf{H}_{fm}$ . Then, we crop the aligned image to remove holes induced by transformation, and resize it to the original image size. The reference image is also cropped and enlarged at the same rate. In our approach, the cropped regions are very small; thus it does not seriously affect the viewing quality of input.

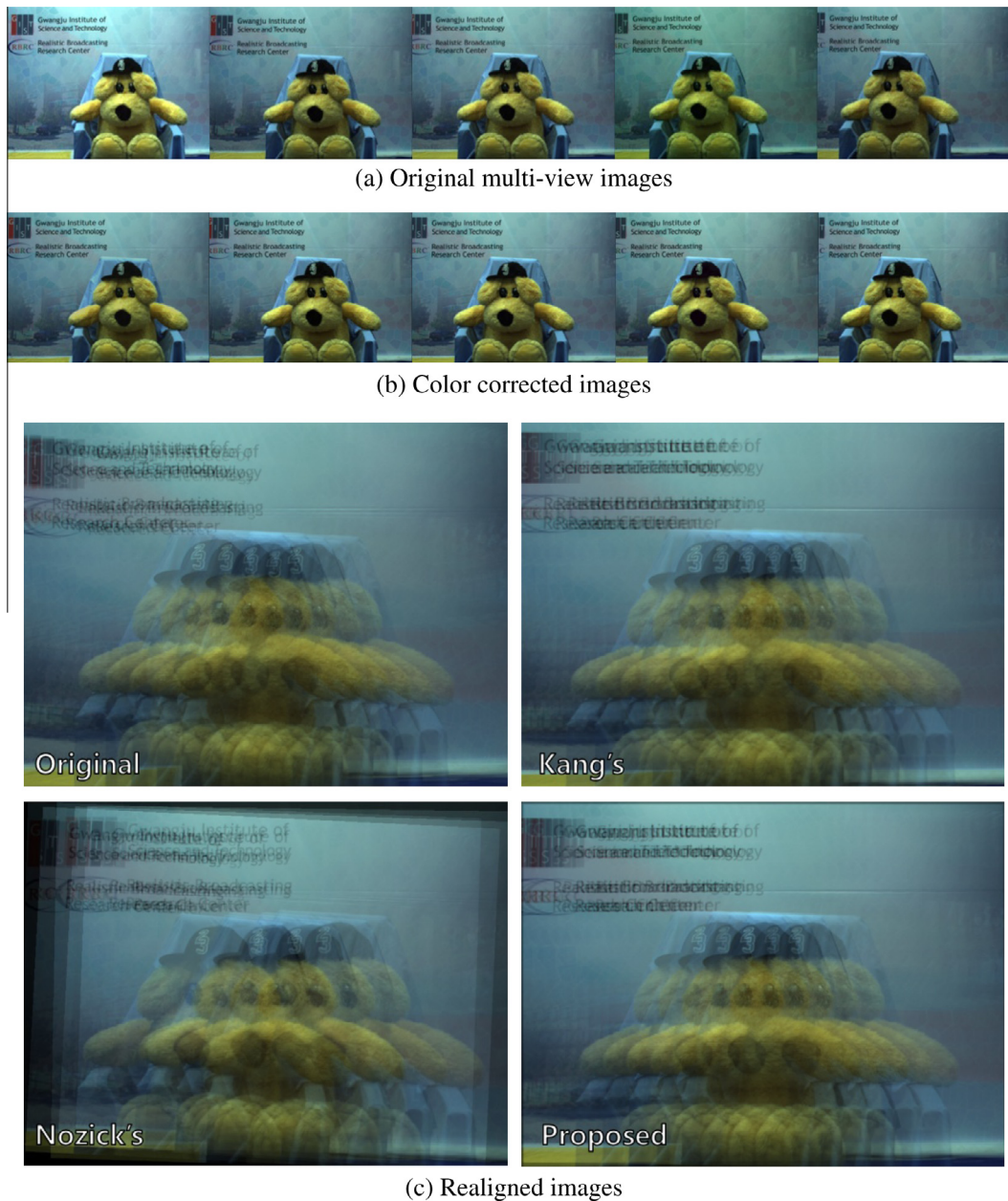


Fig. 12. Final results for bear multi-view images.

## 2.2. Color inconsistency correction

We also correct colorimetric errors in the YUV color domain using the correspondences. The number of the correspondences is enough to estimate the geometric structure but not for analyzing color differences between view pair. In order to supplement color correspondences, we extracted additional samples co-located on the Gaussian-filtered images. In this paper, we use three different Gaussian filters with  $\sigma = \{3, 5, 9\}$  and the kernel aperture is  $50 \times 50$ .

For analyzing the properties of YUV channels, we captured the images with different exposure and color temperature settings. The corresponding relation is shown in Fig. 6. While the Y components nonlinearly changes, the U and V components linearly change.

Therefore we use GOG model for Y component and linear model for U and V components to compensate relative color differences between views. We define three error functions as

$$\begin{aligned}
 Error_Y &= \sum_{i=1}^N w_i (Yr(i) - C_{Y1} Ys(i)^{C_{Y3}} + C_{Y2}) \\
 Error_U &= \sum_{i=1}^N w_i (Ur(i) - C_{U1} Us(i) + C_{U2}) \\
 Error_V &= \sum_{i=1}^N w_i (Vr(i) - C_{V1} Vs(i) + C_{V2})
 \end{aligned} \tag{8}$$

where  $Yr$ ,  $Ur$ , and  $Vr$  are components of the reference view and  $Ys$ ,  $Us$ , and  $Vs$  are components of the source view.  $C$  components are unknowns that need to be estimated from correspondences. These values are normalized from 0 to 1.  $w$  is a weighting factor for each correspondences, and is determined according to the ratio of the occupied area from where the correspondence are extracted. Since SURF does not consider global properties of input pair and extract

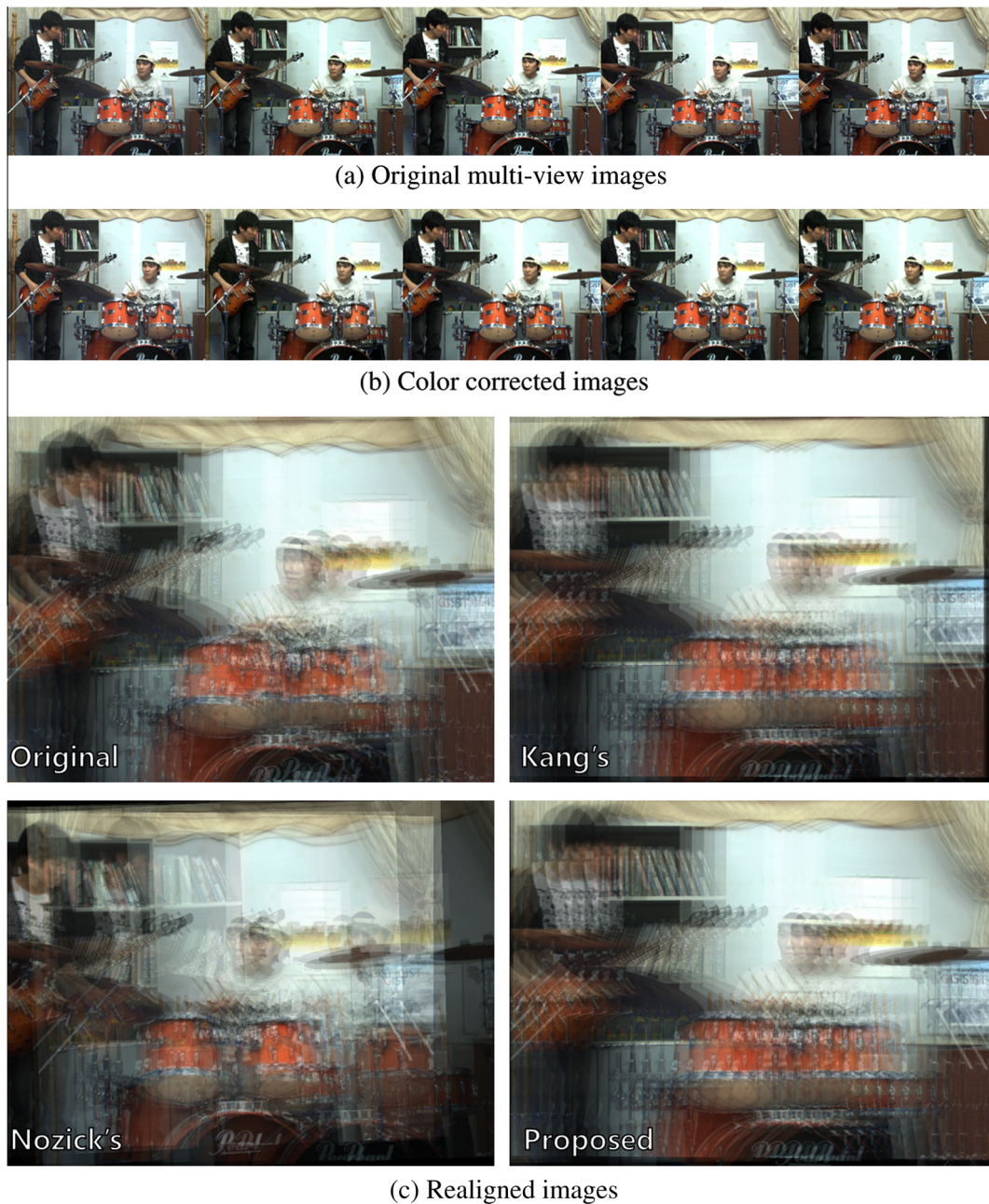


Fig. 13. Final results for *band* multi-view images.

features from locally textured areas, we use  $w$  to weight correspondences whose colors are great important in the inputs.

Fig. 7 demonstrates the original source image, and importance map considering the ratio of occupied areas, and weights for correspondences. With these weights, we estimate the  $C$  components using the LM algorithm.

After estimating each coefficient for luma and chroma components, we convert pixel values of the rearranged source image. For faster execution, we generate lookup tables which possess all intensity values in the dynamic range and their converting values.

### 3. Experimental results

At first, a series of experiments were performed on image pairs to objectively evaluate the performance of the proposed algorithm: *components*, *people*, and *train*. These images were captured under

different camera settings. The overlapped original images are shown in Fig. 8(a). Fig. 8(b) demonstrates the enlarged parts of the red boxed regions, showing not aligned image planes. We applied the proposed and conventional algorithms to these test images.

Fig. 9 shows the geometric error reduction results of Hartley's [16], Fusiello's [19], Nozick's [20], and the proposed algorithms in order. We used the software provided by each author. The bottom part exhibits the enlarged images, and the red horizontal lines are for comparison. The conventional approaches unfold input images to a co-plane and severely distort both images. Nevertheless, the proposed method reduces vertical disparities without significant distortion.

For objective quality measure, correspondences were extracted again after geometric error reduction, and the vertical disparities of the correspondences were averaged. The results are shown in Table 1.

**Table 4**  
Comparison of subjective qualities.

	Bear		Band		Average
	Visual comfort	Naturalness of viewpoint change	Visual comfort	Naturalness of viewpoint change	
Original	4.3	4.6	4.1	4.2	4.3
Kang's	4.6	4.8	4.6	4.8	4.7
Nozick's	4.0	4.2	3.6	3.8	3.9
Proposed	4.5	4.7	4.6	4.7	4.6

In the results, the proposed method decreases vertical disparities by about 86% when compared to the original inputs. Even though the proposed method only transforms one view, its performance stacks up to the performance of the previous rectification that transforms both views.

Especially the proposed algorithm shows notable performance with respect to original image preservation. To measure the degree of distortion, valid pixels in the resulting images were counted. Valid pixels represent pixels with proper values in both the source and reference images at co-located positions. The results are shown in Table 2. While our method can preserve greater than 97% of the pixels, the conventional algorithms lose 7–44% of the pixels; in addition, the resulting images are unnaturally rotated.

Since only rectangular images are usable for multi-view display devices, we cropped the transformed images. After cropping, the valid viewing region becomes much smaller, as shown in Fig. 10. The valid viewing regions of the other algorithms are only 33–84%; however, those of the proposed method are greater than 97%. This means that the geometric compensation of the proposed method can provide more reliable results in practice.

Objective evaluation of color correction algorithms is very difficult. Therefore, we took the test image including a color chart, and compared colors in the chart after applying each algorithm. The proposed algorithm was compared with color transfer [8], histogram matching [9], brightness transfer function [12], camera characteristic [14], and energy function [10,11]. Fig. 11(a) is the input pair, and the following are the corrected source images using each algorithm.

The average of mean absolute error (MSE) values between the color patches of the source and reference images was calculated in the CIE Lab domain. This domain is a standardized linear color space and its Euclidean distance (ED) is closely related to human perception of color differences. As shown in Table 3, the proposed method provides the smallest MSEs and EDs. The energy function also shows low differences but induces distortion in homogeneous regions due to the conflict between energy terms. The proposed algorithm naturally reduces the color inconsistency between the views compared to the other methods.

We applied the proposed algorithm to multi-view images, and the results are demonstrated in Figs. 12 and 13. Related to geometric error reduction, we additionally implemented Kang's multi-view rectification algorithm [15] since Hartley's and Fusiello's algorithms do not support multi-view images. We calibrated all cameras for implementing Kang's method. Figs. 12a and 13a are the original multi-view images, and Figs. 12b and 13b show the color corrected results. The bottom images are results of geometric error compensation. The proposed algorithm successively corrected geometric errors regardless of the view number, and rearranged views to employ uniform view intervals. The performance of Nozick's algorithm highly depended on the input images and the accuracy of correspondences.

Twelve observers participated in the subjective quality assessment. During the assessment, the original and corrected multi-view images were displayed on a multi-view display device in a random fashion. The observers were asked to view the sequences

while changing viewpoints and give scores of two factors (visual comfort and naturalness of viewpoint change) according to the ITU-R BT.500-11 recommendations [27]. The results are shown in Table 4. While the performance of Nozick's algorithm is unstable and insufficient, the proposed algorithm shows comparable results with Kang's method based on camera parameters.

From the experimental results, the proposed method was confirmed to be successive in reducing colorimetric and geometric errors in multi-view images. Even though input images display excessive discrepancy, high quality multi-view images can be generated using the proposed method.

#### 4. Conclusions

In this paper, we have proposed a colorimetric and geometric error reduction algorithm for multi-view image generation. Unlike the conventional methods, the proposed algorithm does not require additional information and cumbersome tasks. In particular, vertical disparities and color variations among views were reduced. Further, image planes were rearranged so that view intervals among neighboring views are uniform. Experimental results showed that the proposed algorithm provided better results than the conventional rectification and color correction algorithms. In addition, the proposed method generated more comfortable multi-view images even though input images possessed excessive discrepancies. The user can expect to easily capture and watch high quality multi-view images via the proposed method.

#### Acknowledgement

This work was supported by the National Research Foundation of Korea (NRF) grant funded by the Korea government (MEST) (No. 2012-0009228).

#### References

- [1] A. Kubota, A. Smolic, M. Magnor, M. Tanimoto, T. Chen, C. Zhang, Multi-view imaging and 3DTV (special issue overview and introduction), *IEEE Signal Processing Mag.* 24 (2007) 10–21.
- [2] DIMENCO, <http://www.dimenco.eu/>.
- [3] LG Display, <http://www.lgdisplay.com/>.
- [4] H.C.O. Li, J. Seo, K. Kham, S. Lee, Measurement of 3D visual fatigue using event-related potential (ERP): 3D oddball paradigm, *3DTV conference: the true vision-capture, transmission and display of 3D video*, IEEE 2008 (2008) 213–216.
- [5] F.L. Kooi, A. Toet, Visual comfort of binocular and 3D displays, *Displays* 25 (2004) 99–108.
- [6] M. Lambooi, M. Fortuin, I. Heynderickx, W. Jsselsteijn, Visual discomfort and visual fatigue of stereoscopic displays: a review, *J. Imaging Sci.* 53 (2009). 30201–30201.
- [7] N. Joshi, B. Wilburn, V. Vaish, M. Levoy, M. Howoritz, Automatic Color Calibration for Large Camera Arrays, *UCSD CSE Tech*, Report CS2005-0821, 2005, pp. 1–4.
- [8] E. Reinhard, M. Adhikhmin, B. Gooch, P. Shirley, Color transfer between images, *IEEE Comput. Graphics Appl.* (2001) 34–41.
- [9] U. Fecker, M. Barkowsky, A. Kaup, Histogram-based prefiltering for luminance and chrominance compensation of multiview video, *IEEE Trans. Circuits Syst. Video Technol.* 18 (2008) 1258–1267.
- [10] K. Yamamoto, M. Kitahara, H. Kimata, T. Yendo, T. Fujii, M. Tanimoto, S. Shimizu, K. Kamikura, Y. Yashima, Multiview video coding using view

- interpolation and color correction, *IEEE Trans. Circuits Syst. Video Technol.* 17 (2007) 1436–1449.
- [11] M. Panahpour Tehrani, A. Ishikawa, S. Sakazawa, A. Koike, Iterative colour correction of multicamera systems using corresponding feature points, *J. Visual Commun. Image Represent.* 21 (2010) 377–391.
- [12] K. Seon Joo, M. Pollefeys, Robust radiometric calibration and vignetting correction, *IEEE Trans. Pattern Anal. Mach. Intell.* 30 (2008) 562–576.
- [13] W. Qi, Y. Pingkun, Y. Yuan, L. Xuelong, Robust color correction in stereo vision, in: *IEEE International Conference on Image Processing*, 2011, pp. 965–968.
- [14] J. Jung, Y. Ho, Color correction algorithm based on camera characteristics for multi-view video coding, *Signal Image Video Process.* (2012) 1–12, <http://dx.doi.org/10.1007/s11760-012-0341-1>.
- [15] Y. Kang, Y. Ho, An efficient image rectification method for parallel multi-camera arrangement, *IEEE Trans. Consum. Electron.* 57 (2011) 1041–1048.
- [16] R.I. Hartley, Theory and practice of projective rectification, *Int. J. Comput. Vision* 35 (1999) 115–127.
- [17] Q.T. Luong, O.D. Faugeras, The fundamental matrix: theory, algorithms, and stability analysis, *Int. J. Comput. Vision* 17 (1996) 43–75.
- [18] J. Mallon, P.F. Whelan, Projective rectification from the fundamental matrix, *Image Vision Comput.* 23 (2005) 643–650.
- [19] A. Fusiello, L. Irsara, Quasi-Euclidean uncalibrated epipolar rectification, in: *International Conference on Pattern Recognition*, 2008, pp. 1–4.
- [20] V. Nozick, Multiple view image rectification, in: *IEEE International Symposium on Access Spaces*, 2011, pp. 277–282.
- [21] X. Wang, R. Klette, B. Rosenhahn, Geometric and photometric correction of projected rectangular pictures, *Image Vision Comput. New Zealand* (2005) 223–228.
- [22] M. Harville, B. Culbertson, I. Sobel, D. Gelb, A. Fitzhugh, D. Tanguay, Practical methods for geometric and photometric correction of tiled projector, in: *Computer Vision and Pattern Recognition Workshop*, IEEE, 2006, pp. 1–8.
- [23] M.S. Brown, Y.C. Tsai, Geometric and shading correction for images of printed materials using boundary, *IEEE Trans. Image Process.* 15 (2006) 1544–1554.
- [24] H. Bay, T. Tuytelaars, L. Gool, SURF: Speeded Up Robust Features, in: A. Leonardis, H. Bischof, A. Pinz (Eds.), *Computer Vision - ECCV 2006*, Springer, Berlin Heidelberg, 2006, pp. 407–417.
- [25] R. Hartley, A. Zisserman, *Library, Multiple View Geometry in Computer Vision*, Cambridge University Press, 2003.
- [26] P.E. Gill, W. Murray, Algorithms for the solution of the nonlinear least-squares problem, *SIAM J. Numer. Anal.* 15 (1978) 977–992.
- [27] I.-R.R. BT.500-11, Methodology for the Subjective Assessment of the Quality of Television Pictures, ITU Technical Report, Geneva, Switzerland, 2002.